



# 1 **Impacts of anthropogenic water regulation on global** 2 **riverine dissolved organic carbon transport**

3 Yanbin You<sup>1,2</sup>, Zhenghui Xie<sup>1,2\*</sup>, Binghao Jia<sup>1</sup>, Yan Wang<sup>3</sup>, Longhuan Wang<sup>1</sup>, Ruichao  
4 Li<sup>1</sup>, Heng Yan<sup>1,2</sup>, Yuhang Tian<sup>1,2</sup>, Si Chen<sup>1,2</sup>

5 <sup>1</sup>State Key Laboratory of Numerical Modeling for Atmospheric Sciences and Geophysical Fluid  
6 Dynamics, Institute of Atmospheric Physics, Chinese Academy of Sciences, Beijing 100029, China

7 <sup>2</sup>College of Earth and Planetary Sciences, University of Chinese Academy of Sciences, Beijing 100049,  
8 China

9 <sup>3</sup>State Key Laboratory of Hydrology-Water Resources and Hydraulic Engineering, Nanjing Hydraulic  
10 Research Institute, Nanjing 210029, China

11 *Correspondence to:* Zhenghui Xie (zxie@lasg.iap.ac.cn)

12 **Abstract.** Anthropogenic water regulation activities, including reservoir interception, surface water  
13 withdrawal, and groundwater extraction, alter riverine hydrologic processes and affect dissolved organic  
14 carbon (DOC) export from land to rivers and oceans. In this study, schemes describing soil DOC leaching,  
15 riverine DOC transport, and anthropogenic water regulation were developed and incorporated into the  
16 Community Land Model 5.0 (CLM 5.0) and the River Transport Model (RTM). Three simulations by the  
17 developed model were conducted on a global scale from 1981 to 2013 to investigate the impacts of  
18 anthropogenic water regulation on riverine DOC transport. The validation results showed that DOC  
19 exports simulated by the developed model were in good agreement with global river observations. The  
20 simulations showed that DOC transport in most rivers was mainly influenced by reservoir interception  
21 and surface water withdrawal, especially in central North America and eastern China. Four major rivers,  
22 including the Danube, Yangtze, Mississippi, and Ganges Rivers, have experienced reduced riverine DOC  
23 flows due to intense water management, with the largest effect occurring in winter and early spring. In  
24 the Danube and Yangtze River basins, the impact in 2013 was four to five times greater than in 1981,  
25 with a retention efficiency of over 50 %. The Ob River basin was almost unaffected. The total impact of  
26 anthropogenic water regulation reduced global annual riverine DOC exports to the ocean by  
27 approximately 13.36 Tg C yr<sup>-1</sup>, and this effect increased from 4.83 % to 6.20 % during 1981–2013,  
28 particularly in the Pacific and Atlantic Oceans.



29 **1. Introduction**

30 Rivers are a pipe linking the two major carbon pools of terrestrial and ocean ecosystems and are one of  
31 the key hubs of the global carbon cycle (Cole et al., 2007). According to the IPCC AR5, terrestrial  
32 ecosystems deliver about 1.7 Pg C per year to rivers through surface and subsurface runoff and about 0.9  
33 Pg C per year to oceans via rivers, of which about 0.21 Pg is dissolved organic carbon (DOC) (Ludwig  
34 et al., 1996). This is equivalent to about 1 % of the global net primary productivity (NPP) of terrestrial  
35 ecosystems (Zhang, 2012). Riverine DOC is a higher reactive organic carbon, is easily decomposed, and  
36 is a direct source of carbon for microbial food webs in rivers and oceans, as well as a source of greenhouse  
37 gas emissions from freshwater systems (Li et al., 2019; Tranvik & Jansson, 2002). It deeply affects the  
38 biogeochemical cycles of rivers and offshore ecosystems. Therefore, it is important to clarify the  
39 transport characteristics of riverine DOC for estimating global carbon budgets.

40 In recent years, anthropogenic water management activities, including reservoir interception, surface  
41 water withdrawal, and groundwater extraction, have intensified the degree of interference with natural  
42 processes on the surface of river basins, altered the hydrological and hydraulic processes of rivers, and  
43 affected material circulation and transportation (Zhang, 2012). For example, extraction from rivers,  
44 reservoirs, and underground aquifers affects hydrological systems, leading to a reduction in subsurface  
45 runoff and eventually to decreased soil DOC leaching (Zeng et al., 2016), whereas activities such as  
46 irrigation can lead to increased surface runoff, resulting in increased soil carbon losses (Ren et al., 2016).  
47 Artificially constructed large reservoirs or dams disrupt the carbon cycle balance of the river continuum  
48 in its natural state (Maavara et al., 2017), resulting in retention of DOC and sediment, while lower river  
49 velocities and higher material concentrations lead to increased microbial activity in the water body, thus  
50 changing the nutrient state of the river ecosystem (Liu et al., 2022). However, the impact of these  
51 anthropogenic disturbances on riverine carbon transport has been ignored in estimating the global carbon  
52 budget (Regnier et al., 2013).

53 Based on field surveys involving global riverine DOC transport flux estimation, the United Nations  
54 Environment Programme has constructed a world river discharge database, GEMS-GLORI, that lists 48  
55 attributes of 555 major world rivers (Meybeck, 1982; Meybeck & Ragu, 2012). There are also regional  
56 survey programs, such as the Pan-Arctic River Transport of Nutrients, Organic Matter, and Suspended  
57 Sediments (PARTNERS, <https://arcticgreativers.org/>) and the United States Geological Survey (USGS)



58 Data Center (<https://waterdata.usgs.gov/nwis>), which provide riverine organic carbon flux data for parts  
59 of large rivers. Field survey studies are directly limited by data availability and completeness and  
60 therefore mostly focus on large rivers in developed regions, making it difficult to cover rivers in other  
61 regions. Moreover, only annual averages are usually available, with no time-series variation. Some  
62 researchers have started to explore the mechanisms of riverine carbon flux changes using empirical  
63 statistical models, which combine observed data with driving factors including river basin characteristics  
64 (Ludwig et al., 1996), soil carbon and nitrogen ratios (Aitkenhead & McDowell, 2000), land-cover types  
65 (Harrison et al., 2005), and river discharge (Fabre et al., 2020). However, the empirical statistical method  
66 does not consider complex ecological processes within the watershed and cannot describe material  
67 changes in the river network in detail. To identify changes in carbon transport and its driving mechanisms  
68 spatially and explicitly, numerous process-based numerical models are currently used for DOC transport  
69 simulations. Futter et al. (2007) proposed the integrated catchments model for carbon (INCA-C), which  
70 explicitly considers land use, hydrological processes, soil carbon biogeochemical cycles, and surface  
71 water processes. Liao et al. (2019) developed a three-dimensional terrestrial ecosystem model (ECO3D)  
72 considering the influence of lateral water flows. These models simulate regional riverine DOC dynamics  
73 more accurately than earlier models, but their accuracy relies on complex parametric schemes of eco-  
74 hydrological processes and extensive data surveys, so that it is difficult to extend these models to global-  
75 scale simulations. Wu et al. (2014) integrated ecological driving factors and biogeochemical processes  
76 to develop a TRIPLEX-DOC model that predicts DOC metabolism, sorption, desorption, and loss  
77 processes in soils. Li et al. (2019) added a river hydrological process module to construct the TRIPLEX-  
78 HYDRA model and applied it to simulate global riverine DOC fluxes. However, the model did not  
79 consider the impact of human activities on riverine DOC transport. Tian et al. (2015) constructed the  
80 dynamic land ecosystem model (DLEM), a fully distributed model that integrates vegetation dynamics  
81 with processes such as water, carbon, nitrogen, and phosphorus cycling and the effects of human activities  
82 and climate change to simulate DOC flux transport in eastern North American rivers. To better quantify  
83 riverine carbon transport processes at watershed scale, Yao et al. (2021) coupled the scale-adaptive water  
84 transport model (Li et al., 2013) to the DLEM model and applied the result to two mid-Atlantic  
85 watersheds in the United States. Nevertheless, these models failed to consider the effects of  
86 anthropogenic water regulation activities. Furthermore, constructing numerical simulation models is a



87 future development direction of riverine carbon flux estimation; at present, models are still not widely  
88 used to simulate riverine carbon transport (Camino-Serrano et al., 2018).

89 In this study, we incorporated global soil and riverine DOC transport schemes considering  
90 anthropogenic water regulation activities into Community Land Model 5.0 (CLM5.0) and conducted  
91 numerical simulations at global scale (spatial resolution of about 1° for the land processes and 0.5° for  
92 the river systems) during 1981–2013 to explore the impact of anthropogenic water regulation activities  
93 on land-to-ocean riverine DOC transport.

## 94 **2. Model Development**

### 95 **2.1. Model Overview**

96 The model was developed based on CLM5.0, which is the land component of the CESM (Community  
97 Earth System Model). CLM is widely used to simulate and study land surface ecohydrological processes,  
98 surface energy exchange processes, and other biogeochemical processes. The latest version of CLM  
99 updates most components of previous versions, explicitly represents land-use and land-cover change,  
100 introduces a revised canopy interception parameterization, and uses the Model for Scale Adaptive River  
101 Transport (MOSART, Li et al., 2013) to replace the original River Transport Model (RTM), in addition  
102 to significant improvements in soil layer resolution, nitrogen cycle, and the snow model. Because the  
103 scale of this study was global, the river transport model still uses linear RTM.

104 However, CLM5.0 lacks an expression of the soil DOC leaching process and the DOC transport and  
105 transformation process in rivers. Therefore, in this paper, schemes for DOC leaching in soils and DOC  
106 transport in rivers will be proposed and incorporated into CLM5.0 to simulate riverine carbon transport.  
107 To investigate the effect of anthropogenic water regulation activities on global riverine DOC transport,  
108 this study used the scheme proposed by Zeng et al. (2016), and coupled it with DOC transport processes.  
109 The model framework is shown in Fig. 1.

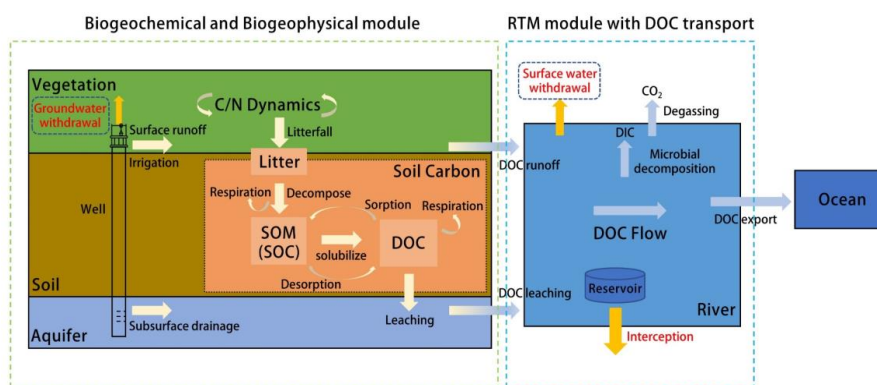


**Figure 1.** Schematic diagram of the land surface model with riverine dissolved organic carbon (DOC) transport and anthropogenic water regulation (C: carbon; N: nitrogen; SOM: soil organic matter; SOC: soil organic carbon; DIC: dissolved inorganic carbon).

## 110 2.2. Soil DOC loss to the river

111 Riverine DOC is mainly derived from organic carbon leaching processes in soil ecosystems in the  
 112 watershed. In CLM5.0, only the leaching process of soil mineral nitrogen is included, and therefore a  
 113 DOC production and loss process was introduced in this study. The soil biochemistry module in CLM5.0  
 114 was constructed based on the Century model (Parton et al., 1988), in which the decomposition of fresh  
 115 litter into soil organic matter is defined as a transformation cascade between the coarse woody debris  
 116 (CWD) pool, the litter pool, and the soil organic matter (SOM) pool. The NPP produced by plants  
 117 eventually enters the soil in the form of litter to constitute the soil carbon pool, accompanied by an  
 118 intervening loss through microbial heterotrophic respiration. Assuming that dissolved organic matter  
 119 (DOM) production is part of the turnover of litter pools and soil organic matter pools and is proportional  
 120 to soil water content, DOC production can be expressed as (Gerber et al., 2010):

$$121 \quad P_{DOC,u \rightarrow d} = f_{DOM} \theta CF_{u \rightarrow d}, \quad (1)$$

122 where  $P_{DOC,u \rightarrow d}$  ( $\text{g C m}^{-2} \text{s}^{-1}$ ) is the DOC flux from the decomposition process;  $f_{DOM}$  is the fraction  
 123 that enters the soil DOM pool;  $\theta$  ( $\text{m}^3 \text{m}^{-3}$ ) is the soil water content; and  $CF_{u \rightarrow d}$  ( $\text{g C m}^{-2} \text{s}^{-1}$ ) is the  
 124 carbon flux from upstream to downstream carbon pools in the decomposition cascade.

125 Soil organic carbon remaining after plant growth and soil respiration is subject to loss as a dissolved  
 126 component leaching from the soil column. The leaching flux depends on the DOC concentration in the  
 127 soil water solution ( $[DOC]$ ,  $\text{g C kgH}_2\text{O}^{-1}$ ) and the hydrologic discharge rate from the soil column to  
 128 streamflow ( $Q_{dis}$ ,  $\text{kgH}_2\text{O m}^{-2} \text{s}^{-1}$ ):



$$129 \quad \text{DOC}_{leached} = [\text{DOC}]Q_{dis}k_{adsorb} - SR, \quad (2)$$

130 where  $[\text{DOC}]$  is calculated as:

$$131 \quad [\text{DOC}] = \frac{NS_{DOC}}{WS_{tot\_soil}}, \quad (3)$$

132 where  $WS_{tot\_soil}$  ( $\text{kgH}_2\text{O m}^{-2}$ ) is the total mass of soil water content integrated over the soil column and

133  $NS_{DOC}$  ( $\text{g C m}^{-2}$ ) is the DOC in the soil pool.

134 Soil DOC readily complexes with metal ions in the soil and forms soil agglomerates, which enable  
 135 soil DOC to be adsorbed onto soil particles. The DOC adsorption coefficients can be estimated as (Li et  
 136 al., 2019; Neff & Asner, 2001):

$$137 \quad k_{adsorb} = \frac{X_i}{X_i + RE}, \quad (4)$$

$$138 \quad RE = mX_i - b, \quad (5)$$

139 where  $X_i$  ( $\text{mg g soil}^{-1}$ ) represents the initial DOC concentration and  $m$  (dimensionless coefficient) and  $b$   
 140 ( $\text{mg g soil}^{-1}$ ) can be considered as measures of potential DOC sorption and desorption by soil.

141 The soil heterotrophic respiration flux of DOC,  $SR$  ( $\text{g C m}^{-2} \text{ s}^{-1}$ ), is estimated by an empirical function  
 142 (Janssens and Pilegaard, 2003):

$$143 \quad SR = R_{10}Q_{s10}^{\frac{T-10}{10}}, \quad (6)$$

144 where  $T$  ( $^{\circ}\text{C}$ ) is the soil temperature;  $R_{10}$  is the soil heterotrophic respiration flux at a soil temperature of  
 145  $10^{\circ}\text{C}$ ;  $Q_{s10}$  is the soil respiration temperature sensitivity.

146 It is necessary to limit the total DOC leaching flux at each time step so that it does not exceed the total  
 147 amount of DOC:

$$148 \quad \text{DOC}_{leached} = \min\left(\text{DOC}_{leached}, \frac{NS_{DOC}}{\Delta t}\right). \quad (7)$$

### 149 2.3. Riverine DOC transport

150 Soil DOC enters the river network system along with surface and subsurface runoff, where it is lost due  
 151 to processes such as microbial degradation. Therefore, based on the water transport framework, the large-  
 152 scale riverine DOC transport equation can be defined as:

$$153 \quad \frac{dS_{DOC}}{dt} = F_{DOC}^{in} - F_{DOC}^{out} + R_{DOC} + L_{DOC} - k_{doc} * Q_{10}^{\frac{T-20}{10}} * S_{DOC}, \quad (8)$$

154 where  $S_{DOC}$  ( $\text{kg C}$ ) is DOC storage within the current grid cell;  $R_{DOC}$  ( $\text{kg C s}^{-1}$ ) and  $L_{DOC}$  ( $\text{kg C s}^{-1}$ )  
 155 represent soil DOC runoff and leaching;  $k_{doc}$  ( $\text{s}^{-1}$ ) is the DOC decomposition rate in the river;  $Q_{10}$



156 (=2.0) denotes the temperature coefficient;  $t$  ( $^{\circ}\text{C}$ ) represents the river water temperature, which is  
157 calculated by a large-scale river water temperature model (Liu et al., 2020; van Vliet et al., 2012; Yearsley,  
158 2009);  $F_{DOC}^{in}$  ( $\text{kg C s}^{-1}$ ) is the sum of inflows of riverine DOC from neighboring upstream grid cells;  
159 and  $F_{DOC}^{out}$  ( $\text{kg C s}^{-1}$ ) is the riverine DOC flux leaving the current grid cell, which is calculated as follows:

$$160 \quad F_{DOC}^{out} = \frac{v^{DOC}}{d}, \quad (9)$$

161 where  $v$  ( $\text{m s}^{-1}$ ) is the effective riverine flow velocity, which is estimated by a simplified Manning's  
162 equation (Oleson et al., 2013);  $d$  is the Euclidean distance between two adjacent grid-cell centers.

#### 163 2.4. Anthropogenic water regulation

164 Anthropogenic water regulation includes reservoir interception, surface water withdrawal, and  
165 groundwater extraction and use. Because reservoir interception and surface water withdrawal are closely  
166 related, they are together called surface water regulation. This study coupled the global reservoir  
167 operation scheme (Hanasaki et al., 2006) with RTM using the method of Liu et al. (2020) to represent  
168 the interception effect of reservoirs on runoff and solutes. The method assumed that the inflow from the  
169 reservoir was the outflow from the current grid cell. Released flow from the reservoir was adjusted for  
170 specific uses (flood control, irrigation, etc.), and surface withdrawals were deducted from the released  
171 water.

172 Surface water is extracted directly from natural rivers and reservoirs to meet human water demands  
173 (Liu et al., 2020; Wang et al., 2020; Xie et al., 2020):

$$174 \quad S_{sw}' = S_{sw} - q_{sw} \Delta t, \quad (11)$$

175 where  $S_{sw}'$  (mm) is the surface water storage after extraction;  $S_{sw}$  (mm) is the original surface water  
176 storage;  $q_{sw}$  ( $\text{mm s}^{-1}$ ) is the rate of surface water intake;  $\Delta t$  denotes the model time step.

177 The groundwater extraction process can be expressed as (Zeng et al., 2016):

$$178 \quad S_{gw}' = S_{gw} - q_{gw} \Delta t, \quad (12)$$

$$179 \quad h' = h - \frac{q_{gw} \Delta t}{s}, \quad (13)$$

180 where  $S_{gw}$  (mm) is the original unconfined aquifer water storage;  $q_{gw}$  ( $\text{mm s}^{-1}$ ) is the rate of  
181 groundwater pumping;  $h$  (mm) represents the original groundwater table depth;  $s$  is the aquifer-  
182 specific yield;  $S_{gw}'$  (mm) and  $h'$  (mm) denote the aquifer water storage and the groundwater table depth  
183 after pumping.



184 Human water use can be divided into agricultural irrigation water and other industrial and domestic  
185 water, where irrigation water is considered as effective precipitation directly back to the soil surface and  
186 other water is directly added to the model surface runoff and evapotranspiration fluxes in a certain  
187 proportion (Zou et al., 2015). This process can be estimated by the following equations:

$$188 \quad q_{top} = q_{top} + q_{irrig}, \quad (14)$$

$$189 \quad q_{surf} = q_{surf} + 0.3q_{ind} + 0.3q_{dom}, \quad (15)$$

$$190 \quad q_{evap} = q_{evap} + 0.7q_{ind} + 0.7q_{dom}, \quad (16)$$

191 where  $q_{top}$  ( $\text{mm s}^{-1}$ ) is the rate of net water flow entering the soil surface;  $q_{surf}$  and  $q_{evap}$  ( $\text{mm s}^{-1}$ ) are  
192 surface runoff and evaporation; and  $q_{irrig}$ ,  $q_{ind}$ , and  $q_{dom}$  ( $\text{mm s}^{-1}$ ) denote irrigation, industrial, and  
193 domestic water respectively.

#### 194 2.5. DOC transfer induced by water withdrawal and use

195 Anthropogenic water regulation activities also affect DOC transport processes between land and river. It  
196 was assumed here that (1) only the interception effect of reservoirs would be considered, ignoring the  
197 migration transformation process in reservoirs, and the loss rate in reservoirs would be equal to that in  
198 rivers; (2) because groundwater extraction usually occurs *in situ* and will pass through the filtering effect  
199 of the soil layer, the part of DOC that returned to soil with groundwater extraction was ignored; (3) the  
200 loss rate in the process of DOC returning to soil was equal to that in rivers.

201 The process of reservoir interception leading to retention of carbon in rivers can be expressed as:

$$202 \quad F_{DOC,r} = \frac{v(con_r \Delta Q_r)}{d}, \quad (17)$$

203 where  $F_{DOC,r}$  ( $\text{kg C s}^{-1}$ ) denotes the DOC flux retained by the reservoir;  $con_r$  ( $\text{kg C m}^{-3}$ ) is the DOC  
204 concentration in the reservoir;  $\Delta Q_r$  ( $\text{m}^3$ ) is the water volume change in the reservoir.

205 The DOC flux extracted from surface water is calculated based on the intake rate and the solute  
206 concentration in the current grid cell and enters the soil DOC pool after irrigation. The reduction in soil  
207 DOC leaching due to groundwater extraction is then calculated based on soil DOC concentration and  
208 groundwater pumping rate.





209 **3. Data and Experimental Design**

210 **3.1. Data Sources**

211 The climate input forcing data set ( $0.5^\circ \times 0.5^\circ$ ) used for the model proposed in this study was obtained  
212 from CRU-NCEP Version 7 (Viovy, 2018), including air temperature, humidity, incoming solar radiation,  
213 precipitation, surface pressures, and surface winds. The basic land-surface datasets required to drive the  
214 model were set up using the default CLM 5.0 settings with a spatial resolution of  $0.9^\circ \times 1.25^\circ$ ; more  
215 details are available in the technical notes (Lawrence et al., 2018). The global monthly mean atmospheric  
216 CO<sub>2</sub> concentration dataset came from the NOAA/Earth System Research Laboratory  
217 (<https://www.esrl.noaa.gov/gmd/ccgg/trends/global.html>).

218 Reservoir information was obtained from the Global Reservoir and Dam Database (GRanD, Lehner et  
219 al., 2011), containing information on 6,862 dams and their associated reservoirs worldwide, and  
220 interpolated to a spatial resolution of  $0.5^\circ \times 0.5^\circ$ .

221 The human water use activity dataset was derived from the global long-term surface and groundwater  
222 withdrawal dataset estimated by Liu et al. (2020). The dataset has a spatial resolution of  $0.5^\circ \times 0.5^\circ$  and  
223 contains agricultural, industrial, and domestic water demands from 1958 to 2017.

224 **3.2. Observation Data**

225 Because there are few datasets of long time-series observations of DOC fluxes for large global rivers,  
226 annual averages were used to validate the model simulations. The dataset was derived from the database  
227 developed by Dai et al. (2012), which provides discharge and DOC flux observations for sites on the  
228 world's major large rivers. These sites were globally distributed and were influenced by various climatic  
229 and human activities.

230 **3.3. Experimental Design**

231 To investigate the effect of anthropogenic water regulation on DOC transport in rivers, three sets of  
232 simulations were designed using the developed model (Table 1). The first simulation (CTL) was a control  
233 experiment without considering any anthropogenic water regulation activities. The second simulation  
234 (EXPA) only considered surface water regulation, and the last simulation (EXPB) considered all  
235 anthropogenic water regulation. All simulations were run from 1981 to 2013 with a spatial resolution of  
236  $0.9^\circ \times 1.25^\circ$  for the land-surface module and  $0.5^\circ \times 0.5^\circ$  for the RTM. The results were output on a



237 monthly scale. Before the formal numerical simulations, the 1901–1920 atmospheric forcing data cycle  
238 was used to drive the model without any anthropogenic water regulation as the spin-up run to reach an  
239 equilibrium state.

**Table 1.** Experimental design

Name	Period	Surface regulation	Groundwater regulation
CTL	1981–2013	✘	✘
EXPA	1981–2013	✓	✘
EXPB	1981–2013	✓	✓

## 240 4. Results

### 241 4.1. Model Evaluation

242 Figure 2 shows the spatial distribution of multi-year average soil DOC losses, which are the sum of DOC  
243 surface runoff and subsurface leaching. The results show that the global distribution of soil DOC losses  
244 varied widely, especially in Russia and Southeast Asia, western Africa, and tropical South America,  
245 where the losses exceeded  $18,000 \text{ kg C km}^{-2} \text{ yr}^{-1}$ , whereas low runoff arid regions such as northwestern  
246 China, India, and North Africa had the smallest soil DOC losses. The tropics and the temperate regions  
247 of the Northern Hemisphere were the regions with the highest soil DOC losses, which was generally  
248 consistent with previous studies (Harrison et al., 2005).

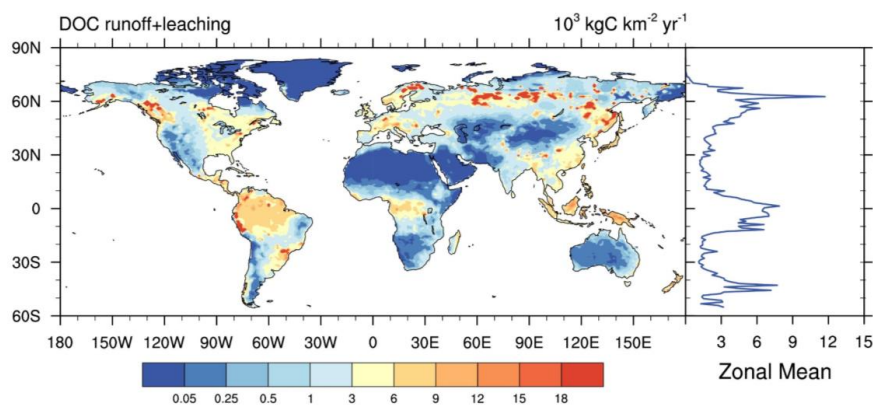


**Figure 2.** Spatial distribution and zonal mean of multi-year average soil DOC losses from 1981 to 2013.

249 The multi-year average river discharges and DOC export fluxes simulated by the developed model



250 were then compared with observed data. Because the model resolution was  $0.5^\circ \times 0.5^\circ$ , only 106 rivers  
251 with watershed areas larger than  $2,500 \text{ km}^2$  were selected. The simulated river discharges were slightly  
252 overestimated (Fig. 3c), but fit well with observations (Fig. 3a) and provided a solid basis for subsequent  
253 simulation of river carbon exports. In addition, the simulated riverine DOC export fluxes tended to be  
254 overestimated in temperate regions and underestimated in the tropics (Fig. 3d), but were close to the 1:1  
255 line compared to the observed DOC fluxes, with  $R^2$  reaching 0.61 and significantly correlated (Fig. 3b).  
256 Moreover, the total global river DOC export fluxes simulated by the proposed model were compared  
257 with the results of previous studies. We estimated that the global terrestrial ecosystem delivers about  
258  $199.78 \text{ Tg}$  of DOC per year to the ocean via rivers, which was in the middle of the values derived from  
259 previous studies (Table 2). Therefore, it could be believed that the model has reasonable accuracy and  
260 can be applied to global-scale riverine DOC export simulation studies.

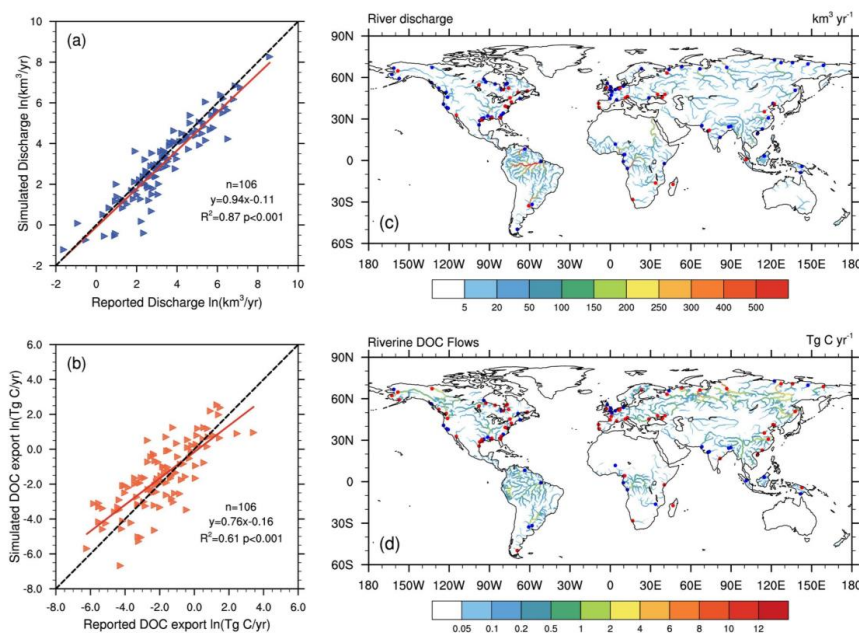


**Figure 3.** Simulated and reported annual (a) river discharge and (b) riverine DOC export flux for 106 global rivers. Spatial distributions of (c) annual discharge and (d) annual riverine DOC exports during 1981–2013. The dots in the map correspond to the locations of the 106 river sites, where blue dots indicate sites that are simulated underestimates and red dots indicate sites that are simulated overestimates.



**Table 2.** Comparison of simulated global total riverine DOC export fluxes with previous studies

Method	DOC (Tg C yr <sup>-1</sup> )	Data Source
GEMS-GLORI	215	Meybeck (1982)
Empirical model	204	Smith & Hollibaugh (1993)
Empirical model	204.81	Ludwig et al. (1996)
Global C: N	361	Aitkenhead & McDowell (2000)
NEWS-DOC	170	Harrison et al. (2005)
Global-NEWS	170	Seitzinger et al. (2005)
Statistical estimation	246	Cai (2011)
TRIPLEX-HYDRA	240	Li et al. (2019)
Empirical model	131.6	Fabre et al. (2020)
CLM5.0-RTM	199.78	This study

261 **4.2. Effects of surface water regulation on riverine DOC transport**

262 The difference between EXPA and CTL was used to obtain the effect of surface water regulation on land  
263 surface hydrological variables. Surface water use has resulted in changes in latent and sensible heat fluxes  
264 in most global irrigation water-using regions (Fig. 4a, 4b), especially in arid or semi-arid regions such as  
265 northern China, India, and the central United States, where latent heat fluxes have increased and sensible  
266 heat fluxes have decreased. Soil and surface temperatures in these regions have also decreased due to the  
267 cooling effect of irrigation (Fig. 4c, 4d). Figure 4e shows that irrigation led to an overall increase in soil  
268 moisture, especially in northern India, Western Europe, and the midwestern United States. In addition,  
269 irrigation also led to an increase in total runoff (Fig. 4f).

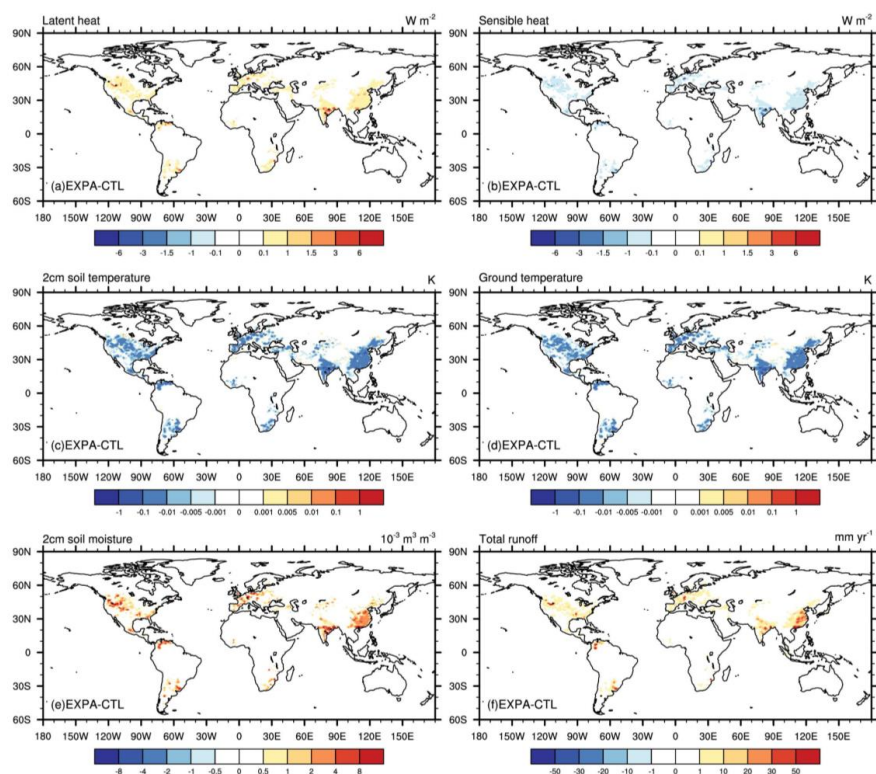


**Figure 4.** Spatial distribution of multi-year average changes in land surface hydrological variables due to surface water regulation from 1981 to 2013: (a) latent heat flux, (b) sensible heat flux, (c) 2 cm soil temperature, (d) surface temperature, (e) 2 cm soil moisture, (f) total runoff. The black dots are the regions that pass the significance  $t$ -test at the 95 % confidence level.

270 Figures 5a and 5b display the effects of surface water regulation on soil carbon losses. Specifically,  
271 the hotspots of significantly increased surface DOC runoff were in areas of high agricultural influence,  
272 such as the central United States, northern India, and northern and eastern China, reaching up to 2,000  
273  $\text{kg C km}^{-2} \text{ yr}^{-1}$ , but the increase in subsurface leaching was relatively small. This may have been the case  
274 because surface water withdrawals from rivers and reservoirs were returned to the soil by irrigation,  
275 bringing back some DOC, directly increasing surface runoff, and also increasing subsurface runoff, and  
276 thus increasing soil DOC losses.

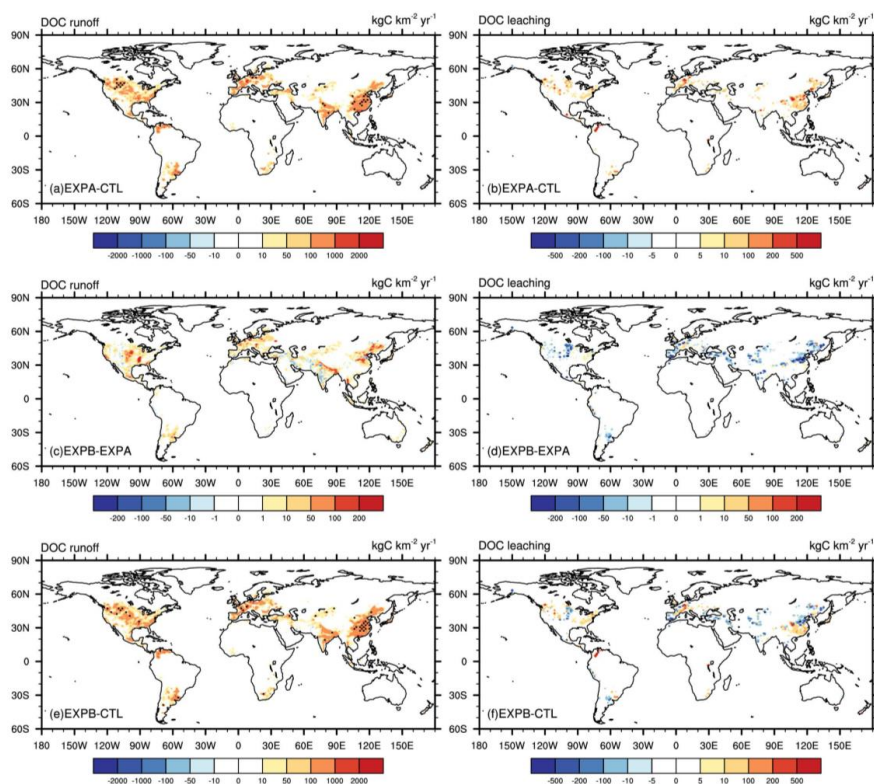


**Figure 5.** Spatial distribution of multi-year average changes in soil carbon losses due to surface water regulation (a, b), groundwater regulation (c, d), and anthropogenic water regulation (e, f) from 1981 to 2013. The black dots are the regions that pass the significance *t*-test at the 95 % confidence level.

277 From Fig. 6a and Fig. 6b, surface water regulation had a significant effect on river discharge and  
278 riverine DOC flow. The combined effects of reservoir interception and surface water withdrawal reduced  
279 the discharge and DOC export of most rivers globally, with significant reductions of more than 50 Gg C  
280  $\text{yr}^{-1}$  in the Yangtze, Yellow, Mississippi, and Ganges Rivers and in some basins in Western Europe. Some  
281 rivers in northern South America experienced increased riverine DOC export, but not significantly,  
282 probably because the increase in river flow caused by agricultural irrigation could have been greater than  
283 the decrease caused by surface water regulation.

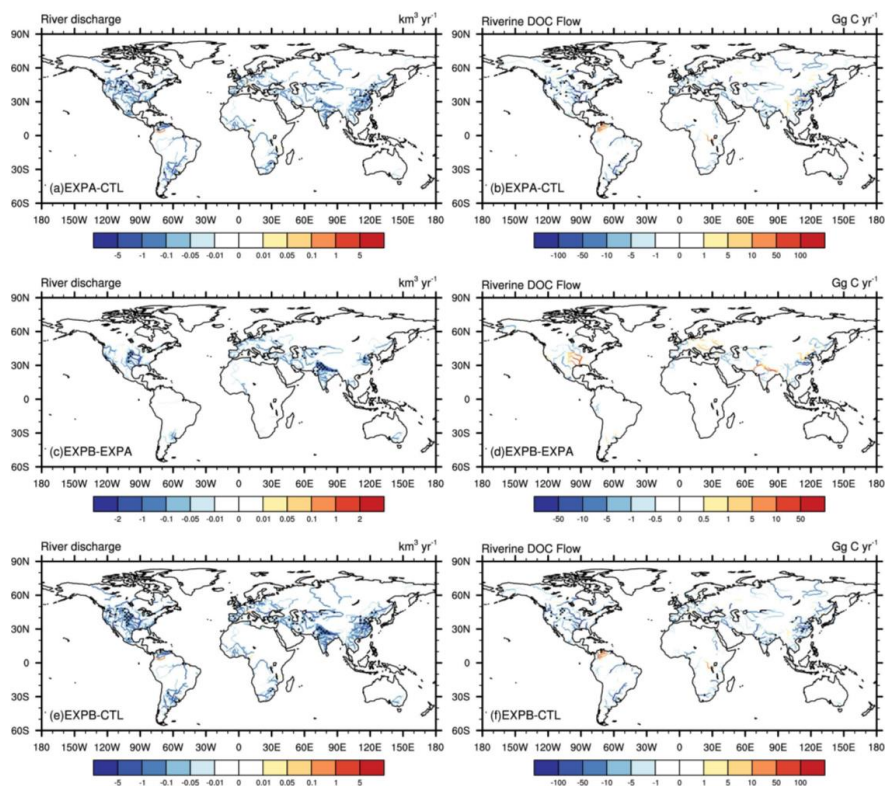


**Figure 6.** Spatial distribution of multi-year average changes in river discharge and riverine DOC flow due to surface water regulation (a, b), groundwater regulation (c, d), and anthropogenic water regulation (e, f) from 1981 to 2013. The black dots are the regions that pass the significance *t*-test at the 95 % confidence level.

284 The blue line in Fig. 7 represents the time-series variation of surface water regulation on global riverine  
285 organic carbon to the ocean. Surface water regulation greatly reduced global riverine DOC transport to  
286 the ocean, from  $-11.1 \text{ Tg yr}^{-1}$  in 1981 to  $-16.4 \text{ Tg yr}^{-1}$  in 2013 (Fig. 7a), with a multi-year average  
287 retention efficiency of about 6 %. This may be related to the fact that reservoir interception increases the  
288 residence time of water and thus increases DOC removal rate (Liu et al., 2022). The regions most affected  
289 by surface water regulation were the Pacific and Atlantic Oceans, and as surface water use in these  
290 regions became more frequent, the reduction in DOC delivery to the ocean was intensified each year.  
291 There was no significant change in the Arctic Ocean region, which may have been due to less  
292 anthropogenic disturbance in the alpine region.

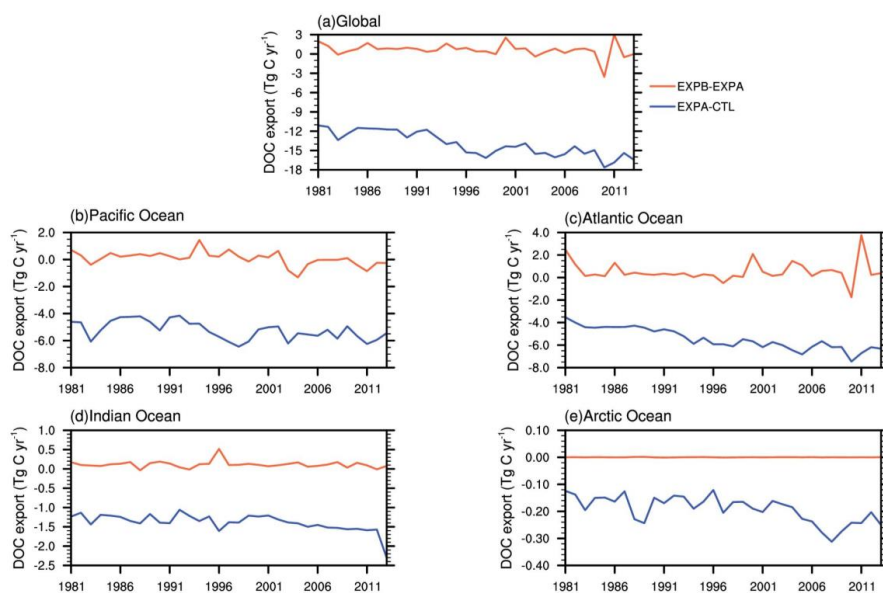


**Figure 7.** Time series of changes in DOC export to oceans due to surface water (blue line) and groundwater regulation (orange line) from 1981 to 2013: (a) global, (b) Pacific Ocean, (c) Atlantic Ocean, (d) Indian Ocean, (e) Arctic Ocean.

293 **4.3. Effects of groundwater regulation on riverine DOC transport**

294 The effects of groundwater regulation on land surface hydrological variables were obtained using the  
295 difference between EXPB and EXPA, as shown in Fig. 8. It can be seen that groundwater extraction  
296 increased latent heat fluxes, decreased sensible heat fluxes, decreased soil and surface temperatures, and  
297 increased soil moisture in most regions of the world. The most significant impacts were in northern China,  
298 northern India, Pakistan, and the central United States, where climate conditions are dry and groundwater  
299 extraction is frequent. Unlike surface water regulation, groundwater extraction has a negative impact on  
300 total runoff (Fig. 8f). Because groundwater is extracted from underground aquifers, whereas surface  
301 water is extracted from rivers and reservoirs, surface water use directly increases total land surface runoff.  
302 However, the impact of groundwater extraction on runoff depends on the groundwater pumping rate,  
303 infiltration rate, and soil evaporation capacity. The increase in latent heat flux leads to an increase in  
304 surface evapotranspiration, which results in a decrease in runoff.



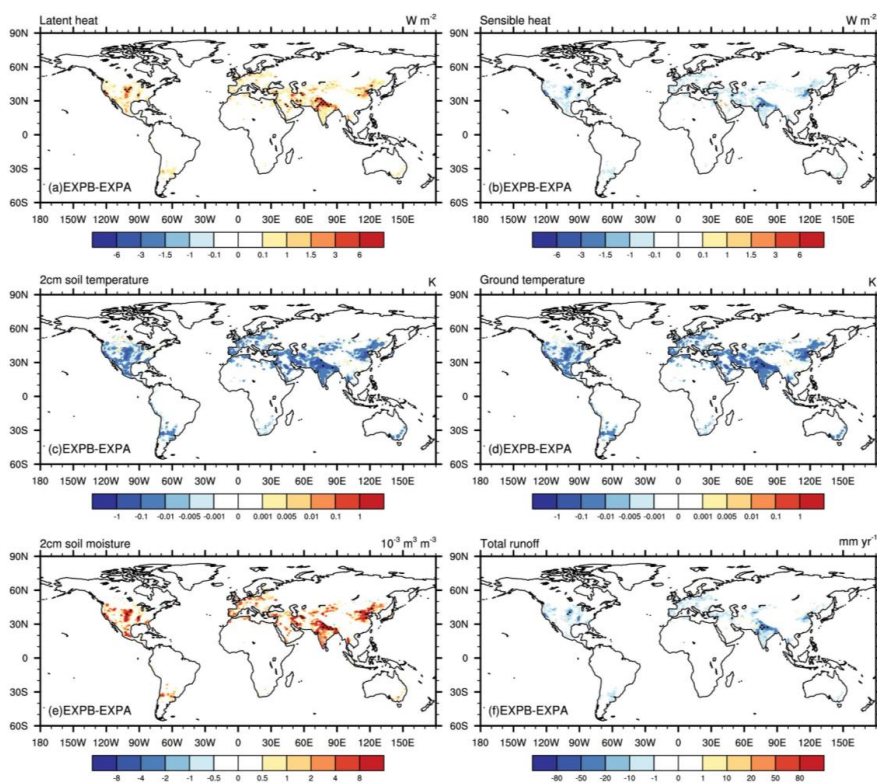


**Figure 8.** Spatial distribution of multi-year average changes in land surface hydrological variables due to groundwater regulation from 1981 to 2013: (a) latent heat flux, (b) sensible heat flux, (c) 2 cm soil temperature, (d) surface temperature, (e) 2 cm soil moisture, (f) total runoff. The black dots are the regions that pass the significance  $t$ -test at the 95 % confidence level.

305 Figures 5c and 5d show the effect of groundwater regulation on soil carbon losses. On the one hand,  
306 extracting water from underground aquifers led to a reduction in subsurface runoff and a consequent  
307 reduction in DOC leaching, especially in northern China and the central United States, where DOC  
308 leaching reductions reached  $200 \text{ kg C yr}^{-1}$ . On the other hand, groundwater irrigation led to an increase  
309 in surface runoff, which led to an increase in DOC runoff. The most affected areas are characterized by  
310 well-developed agriculture.

311 Figures 6c and 6d show the spatial distribution of the effects of groundwater regulation on river  
312 discharge and DOC export from 1981 to 2013. It can be seen that river discharge significantly decreased  
313 in areas with high groundwater extraction rates, such as the central United States, Pakistan, Afghanistan,  
314 and northern China, resulting in a decrease in riverine DOC export. The largest decrease occurred in the



315 Yangtze River Basin in China, reaching 50 Gg C yr<sup>-1</sup>; most other rivers were around 10 Gg C yr<sup>-1</sup>. In  
316 addition, although river discharge was reduced in some river sections, soil DOC loss was higher, and  
317 DOC export fluxes were still increasing, especially in the lower Yellow River, Mississippi River, and  
318 Ganges River basins. This was due to the predominance of agricultural irrigation water in these regions.

319 The amount of carbon flux variation influenced by groundwater regulation was relatively small  
320 compared to that influenced by surface water regulation, but there was some interannual fluctuation, with  
321 the greatest impact during 2009–2012 (Fig. 7). The intermittent increase and decrease of the variation  
322 indicate that river carbon transport fluxes did not decrease directly with increases of groundwater  
323 pumping rate, but were also related to the complex carbon and nitrogen cycling processes in terrestrial  
324 ecosystems. In addition, irrigation after groundwater extraction from an underground aquifer did not  
325 consider directly sending DOC back to the soil carbon pool, and therefore the carbon flux changes were  
326 smaller. Because groundwater regulation activities are mostly concentrated in the northern temperate  
327 zone, the Pacific and Atlantic regions were the most obviously affected, whereas the remaining regions  
328 did not change much.

#### 329 **4.4. Effects of anthropogenic water regulation on riverine DOC transport**

330 This section discusses the combined effects of anthropogenic water regulation on soil and riverine carbon  
331 transport using the EXPB minus CTL results. The effects of anthropogenic water regulation on total  
332 runoff both increased and decreased globally (Fig. 9f). The western United States, Venezuela, and  
333 northern China showed an increase in runoff due to the high intensity of irrigation water use in agriculture.  
334 In contrast, regions such as northern India and the central United States showed a decrease in runoff due  
335 to frequent groundwater extraction. Overall, human water regulation activities led to an increase in latent  
336 heat fluxes and soil moisture and a decrease in sensible heat fluxes and in soil and ground temperatures.

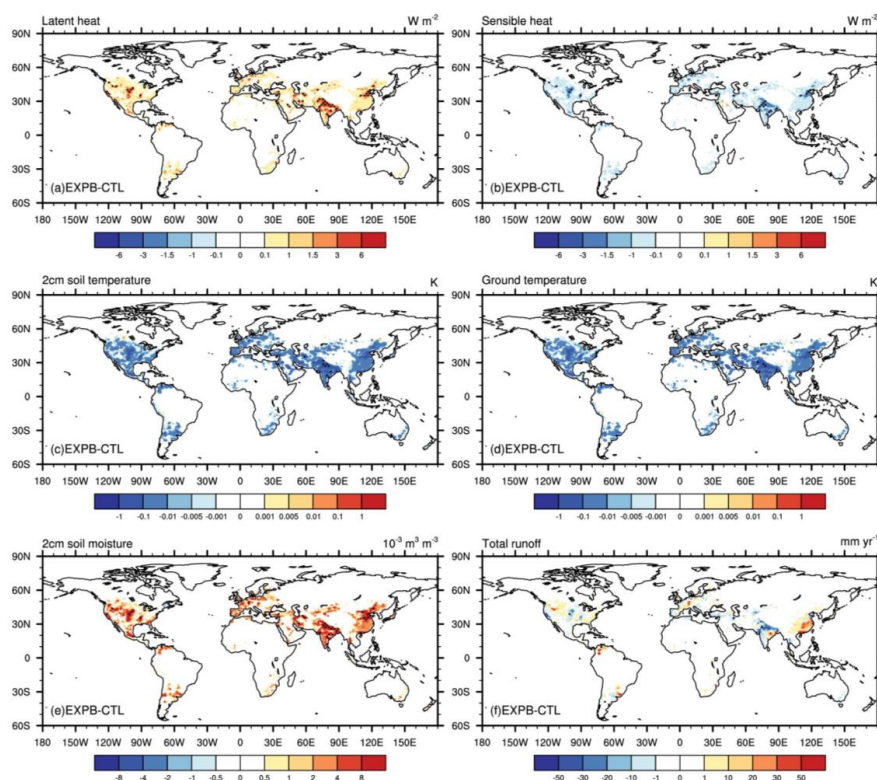


**Figure 9.** Spatial distribution of multi-year average changes in land surface hydrological variables due to anthropogenic water regulation from 1981 to 2013: (a) latent heat flux, (b) sensible heat flux, (c) 2 cm soil temperature, (d) surface temperature, (e) 2 cm soil moisture, (f) total runoff. The black dots are the regions that pass the significance *t*-test at the 95 % confidence level.

337 Figure 5e shows that soil DOC runoff increased, especially in northern China and the midwestern  
338 United States. DOC leaching decreased in some river sections (Fig. 5f), but not significantly. Although  
339 soil DOC runoff showed an overall increase, DOC export fluxes decreased in most rivers globally due to  
340 water regulation (Fig. 6f). On the one hand, human water use activities led to a decrease in river discharge  
341 (Fig. 6e), and on the other hand, reservoir have intercepted part of riverine DOC, which led to an increase  
342 in microbial activity, resulting in a decrease in river carbon flux. In contrast, in the Mississippi and  
343 Ganges River basins, although groundwater regulation increased their DOC export fluxes (Fig. 6d), they  
344 still showed a decrease under the negative feedback effect of surface water regulation, indicating that  
345 most rivers globally are mainly influenced by reservoir interception and surface water withdrawal.

346 Five typical rivers were selected to exhibit how anthropogenic water regulation affects monthly and



347 annual average DOC flows in rivers. The selected rivers were the Mississippi River in the United States,  
348 the Danube River in Europe, the Ob River in Russia, the Yangtze River in China, and the Ganges River  
349 in India. Figure 10 displays the seasonal and interannual variation of DOC flow rates in the five rivers as  
350 calculated by the three sets of simulations respectively. Anthropogenic water regulation had a significant  
351 impact on the Mississippi, Danube, Yangtze, and Ganges Rivers, which decreased significantly in winter  
352 and early spring, whereas the Ob River was almost unaffected. This was the case because of weak water  
353 management activities in the Ob River, whereas the other subtropical and temperate rivers had intense  
354 water management activities and significant seasonal variation in runoff. In addition, only the Mississippi,  
355 Yangtze, and Ganges rivers were affected by minor groundwater regulation, usually occurring during dry  
356 periods, whereas in most seasons, the rivers were affected only by surface water regulation (including  
357 reservoir interception). The annual results showed a significantly strengthening trend of riverine DOC  
358 reduction due to the influence of anthropogenic water regulation, especially in the Danube and Yangtze  
359 Rivers, where the retention percentage in 2013 was four to five times higher than in 1981, up to more  
360 than 50 %, indicating a clear intensification of human water management activities. The influence on the  
361 Mississippi and Ganges Rivers increased slightly and stabilized at about 30–40 %, whereas the influence  
362 on the Ob River was almost 0.

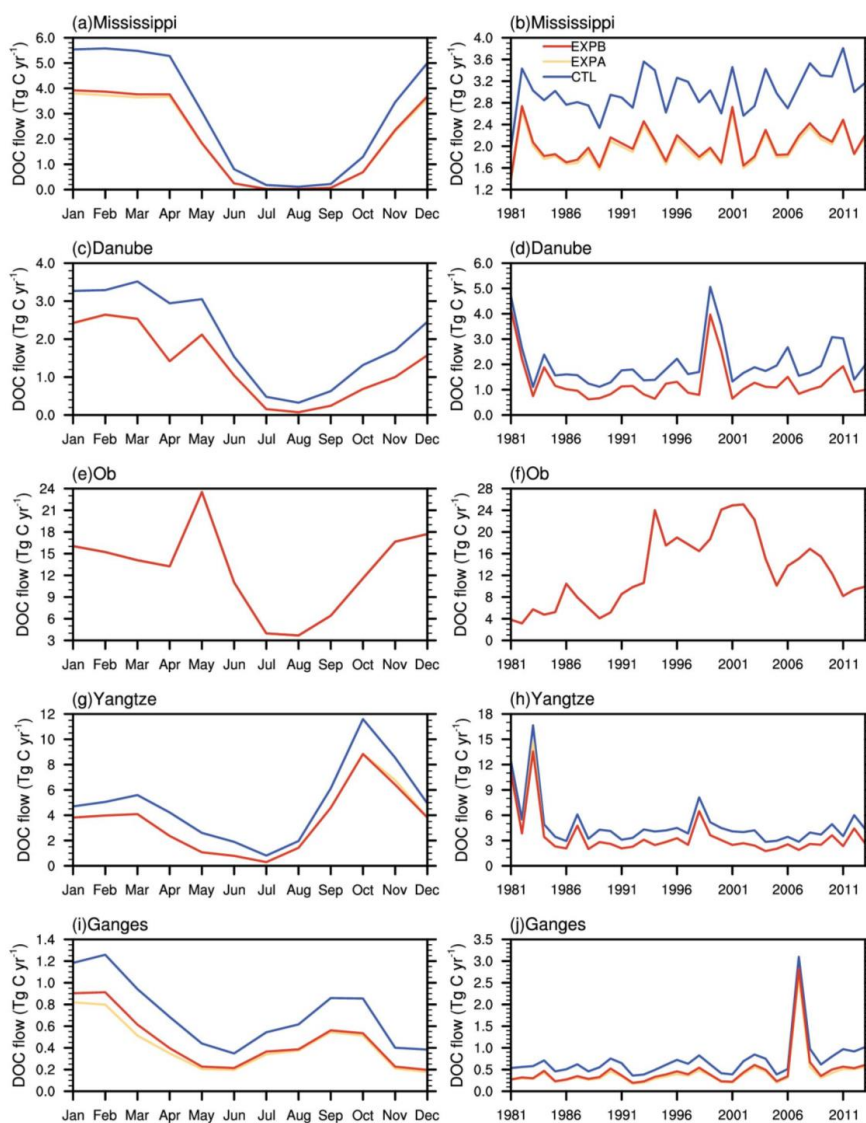


**Figure 10.** Time series of monthly and annual average riverine DOC flow rates for the five typical rivers simulated by CTL (blue line), EXPA (yellow line), and EXPB (red line): (a, b) Mississippi River (32.25° N, 91.25° W), (c, d) Danube River (45.25° N, 28.75° E), (e, f) Ob River (66.25° N, 66.75° E), (g, h) Yangtze River (30.75° N, 117.75° E), (i, j) Ganges River (24.25° N, 88.25° E).

363 Riverine DOC export fluxes have obvious spatial heterogeneity. Six zones were defined according to  
 364 the latitudes where the river mouths are located, and the effects of the presence or absence of  
 365 anthropogenic water regulation on DOC export fluxes are shown in Fig. 11. The hotspot regions of



366 riverine DOC export are concentrated in the tropics (23.5° S–23.5° N) and the mid and high latitudes of  
367 the Northern Hemisphere (40–90° N). The DOC export fluxes of rivers between 40° N and 66° N  
368 accounted for 35.32 % of total global export flux. Due to anthropogenic water regulation, the global DOC  
369 export flux was reduced by 13.36 Tg C yr<sup>-1</sup> compared to the case with no human regulation, with the  
370 greatest impact concentrated in the subtropical and temperate regions of the Northern Hemisphere (23.5–  
371 66° N) because this is the region with the highest intensity of human water use activity.

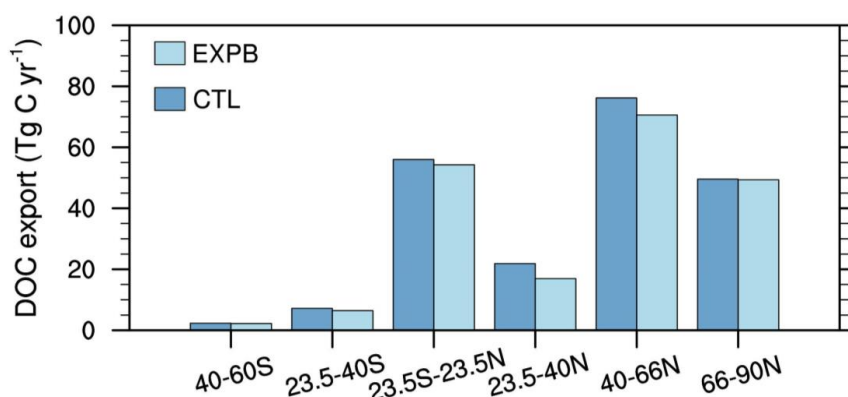


**Figure 11.** Bar chart of latitudinal band distribution of multi-year average DOC export fluxes from 1981 to 2013. Dark blue indicates no human activity, and light blue indicates anthropogenic water regulation.

372 Overall, anthropogenic water regulation reduced global riverine carbon fluxes, and the reduction in  
373 DOC fluxes also intensified over time, from -9.13 Tg C yr<sup>-1</sup> to -16.45 Tg C yr<sup>-1</sup> (Fig. 12), and the  
374 reduction percentage also increased from 4.83 % to 6.20 %. Rivers in the Pacific and Atlantic regions  
375 were more affected by water regulation, and the interannual changes were more consistent with the global  
376 picture. The flux of rivers into the Indian Ocean, which was reduced by water regulation, was about 1.27  
377 Tg C yr<sup>-1</sup>, which was small compared to the global flux, and the flux into the Arctic Ocean was almost  
378 negligible due to the scarcity of human activities.

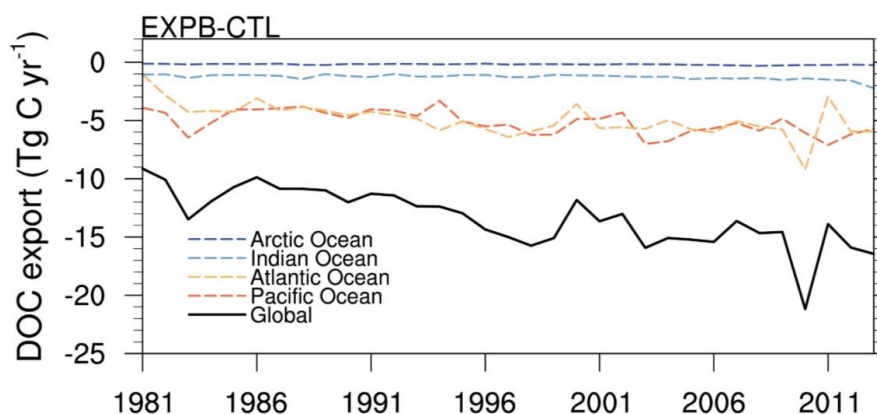


**Figure 12.** Interannual variability in the impact of anthropogenic water regulation on riverine DOC delivery from rivers to the ocean.

379 **5. Conclusions**

380 This study has developed schemes that consider soil and riverine DOC dynamics and anthropogenic  
381 water regulation activities and has incorporated them into the land surface model CLM5.0. The simulated  
382 river discharges and riverine DOC export fluxes were in good agreement with observations obtained for  
383 106 major world rivers. Surface water and groundwater use datasets were used as inputs to the model,  
384 and three sets of numerical simulations were conducted from 1981 to 2013 on a global scale to investigate  
385 the effects of anthropogenic water regulation on riverine DOC transport.

386 The main conclusions of this study are as follows. First, anthropogenic water regulation activities  
387 increased soil losses in most arid and semi-arid regions of the world, although groundwater extraction  
388 reduced subsurface runoff and decreased DOC leaching; however, this decrease was less than the increase  
389 in DOC runoff due to irrigation. Second, the DOC export fluxes of the Yangtze, Yellow, Mississippi, and  
390 Ganges River basins were significantly reduced by reservoir regulation and surface water withdrawal.  
391 However, DOC export fluxes in these areas showed an increase under groundwater regulation, but the  
392 increase was small, indicating that DOC transport in most rivers globally is mainly influenced by  
393 reservoir interception and surface water regulation. Third, further analysis showed that subtropical and  
394 temperate rivers with intensive water management regimes were more affected and that DOC flows  
395 decreased substantially in winter and early spring. The retention percentage has been increasing year by  
396 year, up to over 50 %, indicating a clear intensification of human water management activities, especially



397 along the Danube and Yangtze Rivers. In addition, the greatest impact of anthropogenic water regulation  
398 activities was concentrated in the region from 23.5°N to 66°N because this zone contains the highest  
399 intensity of human water use activities. Fourth, global riverine DOC flux transport to the ocean decreased  
400 by an average of 13.36 Tg C yr<sup>-1</sup> per year due to anthropogenic water regulation activities, and the  
401 decrease in DOC flux became more pronounced with time, from -9.13 Tg C yr<sup>-1</sup> (4.83 %) in 1981 to –  
402 16.45 Tg C yr<sup>-1</sup> (6.20 %) in 2013, especially in the Pacific and Atlantic Ocean regions. Meanwhile, the  
403 Arctic Ocean region was almost unaffected due to low anthropogenic disturbance.

404 In general, this study has developed an effective scheme to simulate DOC export from terrestrial to  
405 aquatic systems, which is important for improving carbon budget estimation and integrated ecosystem  
406 management.

407

408 **Code and Data Availability.** The observed river discharge and riverine DOC exports data can be available  
409 through Dai et al. (2012). The source code of CLM 5.0 is available online  
410 (<https://www.cesm.ucar.edu/models/clm>). The FORTRAN code of developed model in this study is  
411 available upon request. Please contact Zhenghui Xie at [zxie@lasg.iap.ac.cn](mailto:zxie@lasg.iap.ac.cn). The drawing language is the  
412 NCL language.

413

414 **Author contributions.** The scientific framing of this paper was developed by YY, ZX, BJ. The model  
415 was initiated by YY and YW. The literature review was performed by HY, YT and SC. Analyses and  
416 scientific post-processing were performed by LW and RL. All authors discussed the results and  
417 contributed to the writing of the paper.

418

419 **Competing interests.** The contact author has declared that neither they nor their co-authors have any  
420 competing interests.

421

422 **Acknowledgements.** This work was jointly supported by the National Natural Science Foundation of  
423 China (grant number: 41830967), the National Key Research and Development Program of China (grant  
424 number: 2022YFC3201903), and the Youth Innovation Promotion Association CAS (2021073).





425 **References**

- 426 Aitkenhead, J. A. and McDowell, W. H.: Soil C:N ratio as a predictor of annual riverine DOC flux at  
427 local and global scales, *Global Biogeochem. Cycles*, 14, 127–138,  
428 <https://doi.org/10.1029/1999GB900083>, 2000.
- 429 Cai, W.: Estuarine and Coastal Ocean Carbon Paradox: CO<sub>2</sub> Sinks or Sites of Terrestrial Carbon  
430 Incineration?, *Annu. Rev. Mar. Sci.*, 3, 123–145, <https://doi.org/10.1146/annurev-marine-120709-142723>, 2011.
- 432 Camino-Serrano, M., Guenet, B., Luysaert, S., Ciais, P., Bastrikov, V., De Vos, B., Gielen, B., Gleixner,  
433 G., Jorner-Puig, A., Kaiser, K., Kothawala, D., Lauerwald, R., Peñuelas, J., Schrumpf, M., Vicca, S.,  
434 Vuichard, N., Walmsley, D., and Janssens, I. A.: ORCHIDEE-SOM: modeling soil organic carbon  
435 (SOC) and dissolved organic carbon (DOC) dynamics along vertical soil profiles in Europe, *Geosci.  
436 Model Dev.*, 11, 937–957, <https://doi.org/10.5194/gmd-11-937-2018>, 2018.
- 437 Cole, J. J., Prairie, Y. T., Caraco, N. F., McDowell, W. H., Tranvik, L. J., Striegl, R. G., Duarte, C. M.,  
438 Kortelainen, P., Downing, J. A., Middelburg, J. J., and Melack, J.: Plumbing the Global Carbon Cycle:  
439 Integrating Inland Waters into the Terrestrial Carbon Budget, *Ecosystems*, 10, 172–185,  
440 <https://doi.org/10.1007/s10021-006-9013-8>, 2007.
- 441 Dai, M., Yin, Z., Meng, F., Liu, Q., and Cai, W.-J.: Spatial distribution of riverine DOC inputs to the  
442 ocean: an updated global synthesis, *Current Opinion in Environmental Sustainability*, 4, 170–178,  
443 <https://doi.org/10.1016/j.cosust.2012.03.003>, 2012.
- 444 Fabre, C., Sauvage, S., Probst, J.-L., and Sánchez-Pérez, J. M.: Global-scale daily riverine DOC fluxes  
445 from lands to the oceans with a generic model, *Global and Planetary Change*, 194, 103294,  
446 <https://doi.org/10.1016/j.gloplacha.2020.103294>, 2020.
- 447 Futter, M. N., Butterfield, D., Cosby, B. J., Dillon, P. J., Wade, A. J., and Whitehead, P. G.: Modeling the  
448 mechanisms that control in-stream dissolved organic carbon dynamics in upland and forested  
449 catchments: MODELING SURFACE WATER DOC, *Water Resour. Res.*, 43,  
450 <https://doi.org/10.1029/2006WR004960>, 2007.
- 451 Gerber, S., Hedin, L. O., Oppenheimer, M., Pacala, S. W., and Shevliakova, E.: Nitrogen cycling and  
452 feedbacks in a global dynamic land model, *Global Biogeochem. Cycles*, 24,  
453 <https://doi.org/10.1029/2008GB003336>, 2010.



- 454 Hanasaki, N., Kanae, S., and Oki, T.: A reservoir operation scheme for global river routing models,  
455 *Journal of Hydrology*, 327, 22–41, <https://doi.org/10.1016/j.jhydrol.2005.11.011>, 2006.
- 456 Harrison, J. A., Caraco, N., and Seitzinger, S. P.: Global patterns and sources of dissolved organic matter  
457 export to the coastal zone: Results from a spatially explicit, global model: GLOBAL DISSOLVED  
458 ORGANIC MATTER EXPORT, *Global Biogeochem. Cycles*, 19, n/a-n/a,  
459 <https://doi.org/10.1029/2005GB002480>, 2005.
- 460 Janssens, I. A. and Pilegaard, K.: Large seasonal changes in Q<sub>10</sub> of soil respiration in a beech forest:  
461 SHORT-TERM Q<sub>10</sub> OF SOIL RESPIRATION, *Global Change Biology*, 9, 911–918,  
462 <https://doi.org/10.1046/j.1365-2486.2003.00636.x>, 2003.
- 463 Lawrence, D., Fisher, R., and Koven, C.: Technical Description of version 5.0 of the Community Land  
464 Model (CLM), NCAR, NCAR, Boulder, US, 2018.
- 465 Lehner, B., Liermann, C. R., Revenga, C., Vörösmarty, C., Fekete, B., Crouzet, P., Döll, P., Endejan, M.,  
466 Frenken, K., Magome, J., Nilsson, C., Robertson, J. C., Rödel, R., Sindorf, N., and Wisser, D.: High-  
467 resolution mapping of the world’s reservoirs and dams for sustainable river-flow management,  
468 *Frontiers in Ecology and the Environment*, 9, 494–502, <https://doi.org/10.1890/100125>, 2011.
- 469 Li, H., Wigmosta, M. S., Wu, H., Huang, M., Ke, Y., Coleman, A. M., and Leung, L. R.: A Physically  
470 Based Runoff Routing Model for Land Surface and Earth System Models, *Journal of*  
471 *Hydrometeorology*, 14, 808–828, <https://doi.org/10.1175/JHM-D-12-015.1>, 2013.
- 472 Li, M., Peng, C., Zhou, X., Yang, Y., Guo, Y., Shi, G., and Zhu, Q.: Modeling Global Riverine DOC Flux  
473 Dynamics From 1951 to 2015, *J. Adv. Model. Earth Syst.*, 11, 514–530,  
474 <https://doi.org/10.1029/2018MS001363>, 2019.
- 475 Liao, C., Zhuang, Q., Leung, L. R., and Guo, L.: Quantifying Dissolved Organic Carbon Dynamics Using  
476 a Three-Dimensional Terrestrial Ecosystem Model at High Spatial-Temporal Resolutions, *J. Adv.*  
477 *Model. Earth Syst.*, 11, 4489–4512, <https://doi.org/10.1029/2019MS001792>, 2019.
- 478 Liu, S., Xie, Z., Liu, B., Wang, Y., Gao, J., Zeng, Y., Xie, J., Xie, Z., Jia, B., Qin, P., Li, R., Wang, L., and  
479 Chen, S.: Global river water warming due to climate change and anthropogenic heat emission, *Global*  
480 *and Planetary Change*, 193, 103289, <https://doi.org/10.1016/j.gloplacha.2020.103289>, 2020.
- 481 Liu, S., Maavara, T., Brinkerhoff, C. B., and Raymond, P. A.: Global Controls on DOC Reaction Versus  
482 Export in Watersheds: A Damköhler Number Analysis, *Global Biogeochemical Cycles*, 36,



- 483 <https://doi.org/10.1029/2021GB007278>, 2022.
- 484 Ludwig, W., Probst, J.-L., and Kempe, S.: Predicting the oceanic input of organic carbon by continental  
485 erosion, *Global Biogeochem. Cycles*, 10, 23–41, <https://doi.org/10.1029/95GB02925>, 1996.
- 486 Maavara, T., Lauerwald, R., Regnier, P., and Van Cappellen, P.: Global perturbation of organic carbon  
487 cycling by river damming, *Nat Commun*, 8, 15347, <https://doi.org/10.1038/ncomms15347>, 2017.
- 488 Meybeck, M.: Carbon, nitrogen, and phosphorus transport by world rivers, *American Journal of Science*,  
489 282, 401–450, <https://doi.org/10.2475/ajs.282.4.401>, 1982.
- 490 Meybeck, M. and Ragu, A.: GEMS-GLORI world river discharge database,  
491 <https://doi.org/10.1594/PANGAEA.804574>, 2012.
- 492 Neff, J. C. and Asner, G. P.: Dissolved Organic Carbon in Terrestrial Ecosystems: Synthesis and a Model,  
493 *Ecosystems*, 4, 29–48, <https://doi.org/10.1007/s100210000058>, 2001.
- 494 Oleson, K. W., Lawrence, D. M., and Bonan, G. B.: Technical Description of version 4.5 of the  
495 Community Land Model (CLM), NCAR, NCAR, Boulder, US, 2013.
- 496 Parton, W. J., Stewart, J. W. B., and Cole, C. V.: Dynamics of C, N, P and S in Grassland Soils: A Model,  
497 *Biogeochemistry*, 5, 109–131, <https://doi.org/10.1007/BF02180320>, 1988.
- 498 Regnier, P., Friedlingstein, P., Ciais, P., Mackenzie, F. T., Gruber, N., Janssens, I. A., Laruelle, G. G.,  
499 Lauerwald, R., Luyssaert, S., Andersson, A. J., Arndt, S., Arnosti, C., Borges, A. V., Dale, A. W.,  
500 Gallego-Sala, A., Godd ris, Y., Goossens, N., Hartmann, J., Heinze, C., Ilyina, T., Joos, F., LaRowe,  
501 D. E., Leifeld, J., Meysman, F. J. R., Munhoven, G., Raymond, P. A., Spahni, R., Suntharalingam, P.,  
502 and Thullner, M.: Anthropogenic perturbation of the carbon fluxes from land to ocean, *Nature Geosci*,  
503 6, 597–607, <https://doi.org/10.1038/ngeo1830>, 2013.
- 504 Ren, W., Tian, H., Cai, W.-J., Lohrenz, S. E., Hopkinson, C. S., Huang, W.-J., Yang, J., Tao, B., Pan, S.,  
505 and He, R.: Century-long increasing trend and variability of dissolved organic carbon export from the  
506 Mississippi River basin driven by natural and anthropogenic forcing: Export of DOC from the  
507 Mississippi River, *Global Biogeochem. Cycles*, 30, 1288–1299,  
508 <https://doi.org/10.1002/2016GB005395>, 2016.
- 509 Seitzinger, S. P., Harrison, J. A., Dumont, E., Beusen, A. H. W., and Bouwman, A. F.: Sources and  
510 delivery of carbon, nitrogen, and phosphorus to the coastal zone: An overview of Global Nutrient  
511 Export from Watersheds (NEWS) models and their application., *Global Biogeochem. Cycles*, 19,



- 512 <https://doi.org/10.1029/2005GB002606>, 2005.
- 513 Smith, S. V. and Hollibaugh, J. T.: Coastal metabolism and the oceanic organic carbon balance, *Rev.*  
514 *Geophys.*, 31, 75–89, <https://doi.org/10.1029/92RG02584>, 1993.
- 515 Tian, H., Yang, Q., Najjar, R. G., Ren, W., Friedrichs, M. A. M., Hopkinson, C. S., and Pan, S.:  
516 Anthropogenic and climatic influences on carbon fluxes from eastern North America to the Atlantic  
517 Ocean: A process-based modeling study, *J. Geophys. Res. Biogeosci.*, 120, 757–772,  
518 <https://doi.org/10.1002/2014JG002760>, 2015.
- 519 Tranvik, L. J. and Jansson, M.: Terrestrial export of organic carbon, *Nature*, 415, 861–862,  
520 <https://doi.org/10.1038/415861b>, 2002.
- 521 Viovy, N.: CRUNCEP Version 7 - Atmospheric Forcing Data for the Community Land Model,  
522 <https://doi.org/10.5065/PZ8F-F017>, 2018.
- 523 van Vliet, M. T. H., Yearsley, J. R., Franssen, W. H. P., Ludwig, F., Haddeland, I., Lettenmaier, D. P., and  
524 Kabat, P.: Coupled daily streamflow and water temperature modelling in large river basins, *Hydrology*  
525 *and Earth System Sciences*, 16, 4303–4321, <https://doi.org/10.5194/hess-16-4303-2012>, 2012.
- 526 Wang, Y., Xie, Z., Liu, S., Wang, L., Li, R., Chen, S., Jia, B., Qin, P., and Xie, J.: Effects of Anthropogenic  
527 Disturbances and Climate Change on Riverine Dissolved Inorganic Nitrogen Transport, *Journal of*  
528 *Advances in Modeling Earth Systems*, 12, e2020MS002234, <https://doi.org/10.1029/2020MS002234>,  
529 2020.
- 530 Wu, H., Peng, C., Moore, T. R., Hua, D., Li, C., Zhu, Q., Peichl, M., Arain, M. A., and Guo, Z.: Modeling  
531 dissolved organic carbon in temperate forest soils: TRIPLEX-DOC model development and validation,  
532 *Geosci. Model Dev.*, 7, 867–881, <https://doi.org/10.5194/gmd-7-867-2014>, 2014.
- 533 Xie, Z., Wang, L., Wang, Y., Liu, B., Li, R., Xie, J., Zeng, Y., Liu, S., Gao, J., Chen, S., Jia, B., and Qin,  
534 P.: Land Surface Model CAS-LSM: Model Description and Evaluation, *Journal of Advances in*  
535 *Modeling Earth Systems*, 12, e2020MS002339, <https://doi.org/10.1029/2020MS002339>, 2020.
- 536 Yao, Y., Tian, H., Pan, S., Najjar, R. G., Friedrichs, M. A. M., Bian, Z., Li, H., and Hofmann, E. E.:  
537 Riverine Carbon Cycling Over the Past Century in the Mid-Atlantic Region of the United States, *J*  
538 *Geophys Res Biogeosci.*, 126, <https://doi.org/10.1029/2020JG005968>, 2021.
- 539 Yearsley, J.: A semi-Lagrangian water temperature model for advection-dominated river systems, *Water*  
540 *Resources Research - WATER RESOUR RES.*, 45, <https://doi.org/10.1029/2008WR007629>, 2009.



- 541 Zeng, Y., Xie, Z., Yu, Y., Liu, S., Wang, L., Zou, J., Qin, P., and Jia, B.: Effects of anthropogenic water  
542 regulation and groundwater lateral flow on land processes, *Journal of Advances in Modeling Earth*  
543 *Systems*, 8, 1106–1131, <https://doi.org/10.1002/2016MS000646>, 2016.
- 544 Zhang, Y.: The review of the research of the riverine organic carbon cycle, *Journal of Henan Polytechnic*  
545 *University( Natural Science)*, 31, 344–351, <https://doi.org/10.16186/j.cnki.1673-9787.2012.03.006>,  
546 2012.
- 547 Zou, J., Xie, Z., Zhan, C., Qin, P., Sun, Q., Jia, B., and Xia, J.: Effects of anthropogenic groundwater  
548 exploitation on land surface processes: A case study of the Haihe River Basin, northern China, *Journal*  
549 *of Hydrology*, 524, 625–641, <https://doi.org/10.1016/j.jhydrol.2015.03.026>, 2015.
- 550